Surgical Endoscopy (2019) 33:567–575
https://doi.org/10.1007/s00464-018-6332-8

Implementation of 3D printed superior mesenteric vascular models for surgical planning and/or navigation in right colectomy with extended D3 mesenterectomy: comparison of virtual and physical models to the anatomy found at surgery

Javier A. Luzon[1,2] · Bjarte T. Andersen[3] · Bojan V. Stimec[4] · Jean H. D. Fasel[4] · Arne O. Bakka[1,2] · Airazat M. Kazaryan[2,5] · Dejan Ignjatovic[1,2]

Received: 7 March 2018 / Accepted: 6 July 2018 / Published online: 16 July 2018

Abstract

Background Three-dimensional (3D) printing technology has recently been well approved as an emerging technology in various fields of medical education and practice; e.g., there are numerous studies evaluating 3D printouts of solid organs. Complex surgery such as extended mesenterectomy imposes a need to analyze also the accuracy of 3D printouts of more mobile and complex structures like the diversity of vascular arborization within the central mesentery. The objective of this study was to evaluate the linear dimensional anatomy landmark differences of the superior mesenteric artery and vein between (1) 3D virtual models, (2) 3D printouts, and (3) peroperative measurements.

Methods The study included 22 patients from the ongoing prospective multicenter trial "Safe Radical D3 Right Hemicolectomy for Cancer through Preoperative Biphasic MDCT Angiography," with preoperative CT and peroperative measurements. The patients were operated in Norway between January 2016 and 2017. Their CT datasets underwent 3D volume rendering and segmentation, and the virtual 3D model produced was then exported for stereolithography 3D printing.

Results Four parameters were measured: distance between the origins of the ileocolic and the middle colic artery, distance between the termination of the gastrocolic trunk and the ileocolic vein, and the calibers of the middle colic and ileocolic arteries. The inter-arterial distance has proven a strong correlation between all the three modalities implied (Pearson's coefficient 0.968, 0.956, 0.779, respectively), while inter-venous distances showed a weak correlation between peroperative measurements and both virtual and physical models.

Conclusion This study showed acceptable dimensional inter-arterial correlations between 3D printed models, 3D virtual models and authentic soft tissue anatomy of the central mesenteric vessels, and weaker inter-venous correlations between all the models, reflecting the highly variable nature of veins in situ.

Keywords 3-Dimensional printing · Surgical anatomy · Image-guided surgery · Colorectal surgery · Personalized medicine · Patient-specific computational modeling

Additive manufacturing, rapid prototyping, or most commonly referred to as 3D printing, has attracted the attention of the medical world with its rapid technology advances, its increasing availability, and decreasing costs. Nowadays, a desktop 3D printer has become accessible to not only multiple professional fields but also the general consumer [1]. In surgery, physical models have been a tool for anatomical studies and training even before 3D printers were widely available [2–4]. Nevertheless, the modern surgeon predominantly relies on two-dimensional preoperative radiologic datasets, thus limiting an accurate comprehensive view of

This paper was presented and awarded as one of the seven best original oral presentations during the Gerhard Buess Technology Award session during the 26th International Congress of the EAES in London, UK, June 30th–May 1st 2018.

Electronic supplementary material The online version of this article (https://doi.org/10.1007/s00464-018-6332-8) contains supplementary material, which is available to authorized users.

✉ Dejan Ignjatovic
dexexer01@hotmail.com

Extended author information available on the last page of the article

the patient's individual anatomy [5]. Now, with the advances of 3D printing technology, it has become possible to manufacture individual models of the patient's own anatomy to assist procedure planning and intraoperative guidance in high-precision surgical scenarios, such as extended mesenterectomy for colon cancer patients. In a literature review from 2015, Malik et al. [6] summarize that there were three main medical areas in which 3D printing technology had been used (a) anatomic models, (b) surgical instruments, and (c) implants and prostheses. At the same time, they conclude that different specialties were at different stages in the use of this technology.

3D printing technology refers to an additive manufacturing process where new material is added to the surface of existing material to create a physical 3D model, layer by layer. Current scientific literature largely mentions three major techniques used for additive manufacturing within medicine: (1) Fused deposition modeling (FDM), (2) Selective laser sintering (SLS), and (3) Stereolithography apparatus (SLA) [7]. Additionally, it is fair to mention the increasing popularity of material jetting (also called PolyJet™ technology) due to its documented dimensional accuracy [8]. While there appears to exist a battle between additive manufacturing technologies, George et al. recently provided data recommending specific printing technologies according to the anatomical structure of interest [9].

Furthermore, previous studies [8] evaluated different rapid prototyping techniques and the degree of dimensional error and reproduction of structures like the mandibular anatomy. A meta-analysis of additive manufacturing in surgery [10] has shown that 20% studies considered morphometric accuracy as unsatisfactory. In our view, the employment of the one and same methodology (3D printer, resin, protocol) can only improve quantitative accuracy and avoid bias. While there are numerous similar studies evaluating 3D printouts of solid organs, there is still a need to study the accuracy of 3D printouts of more frail, mobile, and complex structures, as for example the vascular anatomy in the central mesentery. In this case, extended mesenterectomy in colon cancer surgery requires a comprehensive understanding of the anatomy due to the complex 3D vascular relations hidden within the mesenteric fat [11, 12]. The objective of this study was to evaluate the dimensional error of SLA printouts (physical models), 3D virtual models, and measurements at surgery of distances between arterial origins and venous confluences on the superior mesenteric artery (SMA) and vein (SMV).

Materials and methods

Patients were recruited from the ongoing prospective multicenter trial "Safe Radical D3 Right Hemicolectomy for Cancer through Preoperative Biphasic MDCT Angiography," with ethical committee approval REK 2010/3354 Norway and registration at ClinicalTrials.gov (Identifier: NCT01351714) on May 9, 2011. The patients were operated in Norway between January 2016 and January 2017. All included patients were required to sign an informed consent form. The trial requires, as a prerequisite, both 3D reconstruction of the individual patient anatomy from the preoperative CT dataset and photography of the vascular anatomical configuration including a sterile paper ruler beside the superior mesenteric vessels after vascular dissection is completed. Selection criteria for patient inclusion were therefore based on the quality of the preoperative CT dataset (quality defined as slice thickness not exceeding 1 mm) and the quality of peroperative images (all vessel origins visualized with no significant image distortion). Distances between origins of the ileocolic artery (ICA) and the middle colic artery (MCA), as well as distances between the confluences of the ileocolic vein (ICV) and the gastrocolic trunk of Henle (GTH) were measured. Additionally, MCA and ICA calibers were measured.

Parameters

The following morphometric values were noted for the 3D virtual models, the 3D printed models, and the anatomy found at surgery:

(a) Inter-arterial distances (IAD): distances between arterial origins (MCA and ICA) along the SMA.
(b) Inter-venous distances (IVD): distances between venous confluences (ICV and GTH) along the SMV.
(c) MCA and ICA calibers (MCAcal and ICAcal): measured at the bases of the respective blood vessels.

Intervascular distances were measured at 1 mm from vessel origins, between lower edge of the superior vessel and upper edge of the inferior vessel (cranial–caudal). Calibers were measured 1 mm from vascular origins. Three repeated measurements were calculated to ensure reproducibility of all outcome measures in virtual, physical, and peroperative modalities. Mean values were calculated for further statistical analysis.

Image acquisition and segmentation

The CT datasets were derived from the high-resolution multidetector computed tomography angiography (MDCTA) of the abdomen, according to the protocol already published [12].

In order to obtain preliminary orientation view of the mesenteric arborization, the abdominal CT datasets were first reconstructed through the 3D volume rendering (VR) technique, using the Food and Drug administration

(FDA)-approved Osirix MD v. 8.5.2 64-bit image processing application (Pixmeo, Bernex, Switzerland). The Region of Interest (ROI) on each slice was carefully outlined via pencil and open polygon tools, the outside region erased by pixel revalidation to air, and then segmented in High-Contrast 3DVR with logarithmic table opacity. Further adjustments were made through the contrast/intensity, cube and scissor tools, and the scout 3D model exported as image and QT movie files. This virtually rendered scout model is an obligatory step performed in the preoperative stage for all patients included in our clinical study. Simultaneously, this reconstruction is also used, for orientation purposes, while performing the following semimanual segmentation step in Mimics software.

Image post-processing

The main image analysis was performed using the FDA-approved Mimics Medical image processing software, ver. 19.0.0.347, and 3-matic Medical software, ver. 11.0.0.109, both Windows 7 Ultimate Edition x64 2016 (Materialise NV, Leuven, Belgium). Imported datasets underwent manual thresholding (with profile line) for attributing value to voxels of the vascular tree. Further, the initial mask was cropped, and underwent detailed and minute single and multiple slices editing with interpolation, following the Osirix scout files. Manual editing was facilitated by dynamic region growing, split mask, 3D LiveWire, Morphology operations, and Boolean operation tools. Finally, a 3D object mask for the superior mesenteric vessels was calculated, without any post-editing (smoothing or triangle reduction), in order to preserve the original form and dimensions. Those masks were exported into two different file formats: the STL format (stereolithography format, widely used in most 3D printing software and hardware) and imported into the 3-matic software, as a MXP file (for virtual measuring).

The time for dataset analysis (segmentation, measurement, exportation of the virtual model into STL format) in Mimics and 3-matic varied in relation to the complexity of the anatomy; an average of 2 h per case can be estimated. To interact with the 3D virtual model, please refer to Supplementary material 1.

3D printing

3D printer-compatible STL files produced by our collaborator in Switzerland were electronically mailed to Norway for printing. The Form1+ (Formlabs, Sommerville, MA, USA) SLA printer was selected due to its documented accuracy for producing high-resolution 3D models of small blood vessels from resin-based polymers [9, 13, 14]. The Form1+3D printer uses a 405 nm violet laser to harden photoactive resin. The resin is a mixture of methacrylates, photo activators, pigments, and additives. Printing was performed using the printing software PreForm from Formlabs. The same setup was used (orientation, building platform and support strategies) to produce all models. The resolution in the PreForm software was set to 0.05 mm, support density was 1.00 (no units), and support point size was 0.60 mm. Models were printed with Formlabs photopolymer resin.

This "bottom–up" SLA printer starts by first descending the build platform into the resin tank, and then laser light is sent from below to harden the photoactive resin which then sticks to the build platform slowly ascending from the resin tank as the model is made beneath. As a single layer solidifies, the process repeats until the 3D object is complete.

3D printed model post-processing

When the 3D print is completed, the build platform is removed from the printer. The scraper included with the printer is used to remove the model. The model is then carefully put into a container filled with 90% isopropanol, shook for 2 min, and soaked for 10 min before moving to a second container, again with 90% isopropanol, and left for another 10 min. This step is critical in order to avoid sticky models and deformation of fine physical details. Support structures are detached from the surface of the model by using a support removal tool supplied by Formlabs.

Virtual measurements

The longitudinal, point-to-point parameters, (IAD, IVD) were performed in a twofold manner: (a) with the aid of the Length tool, measuring the length over surface (LoS); and (b) using the Distance tool, measuring the line "as the crow flies" (direct). The calibers were measured using the 3-point Radius tool (Fig. 1). Finally, MXP files were exported as 3D PDFs with annotations (Supplementary material 1).

Physical measurements

Physical measurements taken from 3D printed models were obtained using a flexible copper wire and a sliding electronic digital caliper (Biltema, Sweden). Intervascular distances were obtained through measuring the length of the wire after straightening it out (Fig. 2). Vascular calibers were obtained by direct measurement at vessel origin. All measurements have been done three times and the mean has been used for further statistical analysis.

Peroperative measurements

Peroperative measurements were obtained with a photograph-based approach. A digital camera was positioned perpendicularly (90°) to the patient over the laparotomy

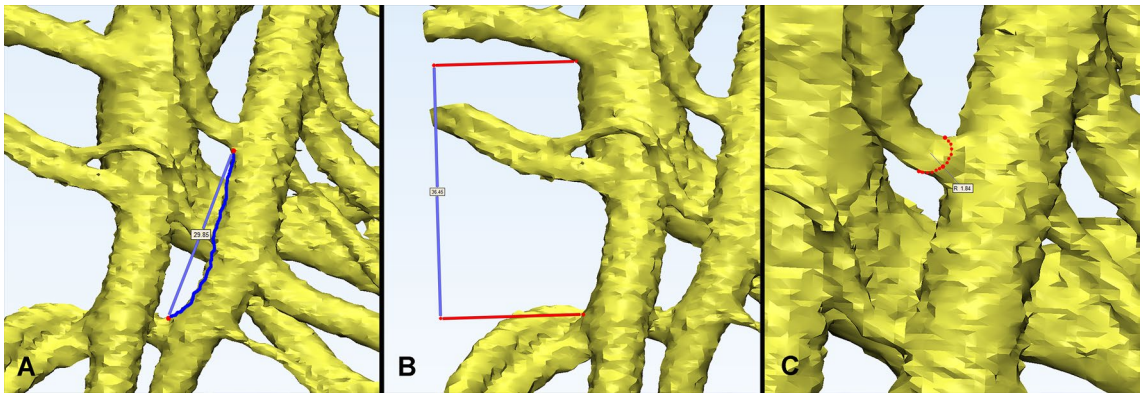

Fig. 1 Virtual measurements methodology taken through 3-matic tools. **A** Inter-arterial distance (IAD), i.e., ileocolic artery-middle colic artery (ICA-MCA) measured with the length over surface (LoS) tool. **B** Inter-venous distance (IVD), i.e., Ileocolic vein-gastrocolic trunk of henle (ICV-GTH) measured with the direct distance tool. **C** Middle colic artery (MCA) caliber measured with the 3-point radius tool

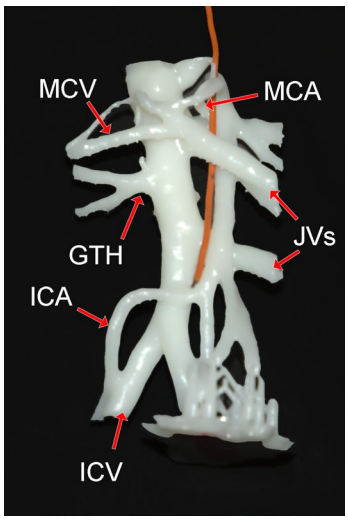

Fig. 2 Physical measurements taken from 3D printed models with a flexible copper wire. Middle colic vein (MCV), middle colic artery (MCA) gastrocolic trunk of henle (GTH) jejunal veins (JVs), ileocolic artery (ICV), ileocolic vein (ICA)

incision. A sterile paper ruler was placed at the level of the central mesenteric vessels. The camera was placed approximately 40 cm away from the abdominal surface. Multiple images were necessary in accordance with the desired exposure of vascular branches and their origins. Synchronization with cardiac cycles and abdominal vessel pulsatility was not taken into consideration during photographing. All photograph-based measurements were obtained by one specific gastrointestinal surgeon (co-author BTA). Peroperative photographs including the imprinted scale were imported into the image editing software ImageJ version 1.6.0 (public domain, National Institutes of Health, Bethesda, MD, USA). This software translates pixels into length. Integrated scaling and calibrating analysis were used in relation to the integrated ruler in the image to perform measurements. The zoom tool was used to enhance precision of measurements. With the summarize tool, the software automatically calculated the mean, standard deviation, and minimum and maximum values from consecutive measurements (Fig. 3).

Statistical analysis

Statistical analyses were accomplished using the Statistica 64-bit data analysis software system, Dell Inc. (2015), Tulsa, USA. Descriptive statistics, Shapiro–Wilk W test of normal distribution, and Pearson correlation test were used for statistical analysis. The probability significance level was set at $p < 0.05$ for W test, and 3-level relationships (strong 0.7, moderate 0.5, and weak 0.3) were applied for the correlation coefficient r.

Results

A total of 22 patients (13 females; mean age 63.1, range 40–81 years) fulfilled the criteria to be included in this study (CT and peroperative image quality). Summary descriptive statistics for all the items analyzed are presented via box & whisker plots (Fig. 4). A high variability, based on the SD values was found in all the 14 displayed groups. Therefore, we performed the Shapiro–Wilk W test for normality for each of them. A significant normal distribution was discovered throughout ($W = 0.915$–0.985, $p = 0.060$–0.989). This was a necessary condition for applying the Pearson's linear bivariate correlation test on all the measured parameters; the results are presented as correlation matrices (Tables 1, 2). From the results presented it clearly emerges that the inter-arterial distances had a strong mutual correlation between

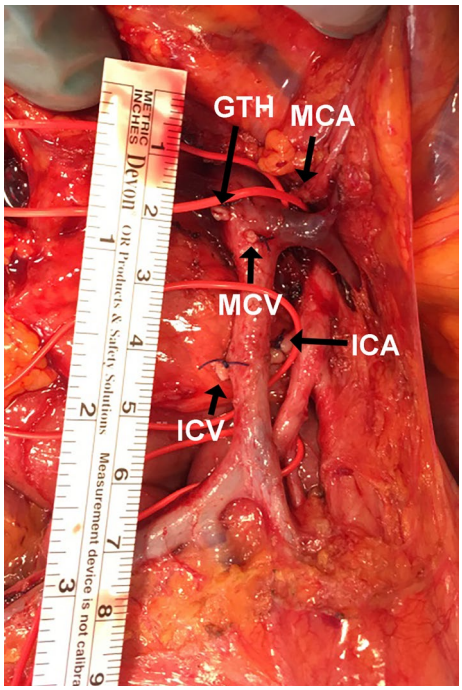

Fig. 3 Peroperative images taken with a sterile paper ruler scaled in mm. Digital measurements of intervascular distances were performed within these photographs. Gastrocolic trunk of henle (GTH), middle colic artery (MCA), middle colic vein (MCV), ileocolic artery (ICA), ileocolic vein (ICV)

all these issues implied: CT (both types of measurement), 3D print model, and peroperative measurements. In this portion of the study, the virtual and physical modes have proven reliability, i.e., to be close to reality (PerOp). Concerning the inter-venous distances, strong manifold correlations were found, between the 2 CT measurements mutually and both the 3D print model, while all their correlations with the peroperative measurements were considered as weak. On the other hand, ICA and MCA calibers showed significant correlation only between the CT and the 3D print measurements; peroperative measurements vs. the former two modalities presented weak or null correlations.

Observations regarding 3D printing

It took between 4 and 6 h to print one model in 1:1 size, using approximately 100 mL resin per sample. In this case, the Form1+ SLA printer was a rather inexpensive printer at the time of purchase in 2014, costing around 3000 USD. Additionally, every 1 L of resin costs around 215 USD. Additional costs are shown in Table 3, thus, each 3D printed model costs roughly 21–34 USD. The printer required continuous maintenance and calibration, which was time consuming. Several models had to be reprinted due to insufficient print quality, increasing both cost and loss of time.

Discussion

The most important finding of this study is that 3D printed models of the central mesenteric vascular anatomy are accurate enough to allow practical 3D anatomical orientation before and during radical D3 right hemicolectomy for cancer. It is equally important to recognize that the central vascular structures (SMA, SMV, and their branches) represent soft/elastic tissue that is mobile within the abdominal cavity and changes in consistency (density) and size (caliber) depending on the blood flow. While all blood vessels are distensible, veins are about eight times more distensible than arteries [15], thus providing a reservoir for storing large quantities of extra blood, which can create variable inter-venous distances, as it was presented in our results. Walls of both arteries and veins have three tunics, called the intima, media, and the adventitia. An artery has a thicker media and relatively narrow lumen in comparison with a vein [16]. Dynamic stretching and volume changing of vessels during surgery, especially veins, are factors that need to be taken into account when searching for measurement correlations. This unique physiological and volumetric characteristic of veins can give an explanation to the weak correlation of inter-venous distances between our virtual and physical models. It is also important to recognize that CT-reconstructed images are based on contrast media (intraluminal measurements) and these values cannot always be accurately correlated with intraoperative values (extraluminal measurements) [17, 18]. As shown in Fig. 4, while intervascular distances did not show any high variability between all the anatomical modalities measured, arterial calibers of 3D printouts had higher values compared to the rest of the models. It is fair to mention that the small metric dimensions (millimeters) used to measure calibers versus centimeters used in intervascular distances can lead to increased data variability. It should be noted that the vascular dissection technique employed was within the vascular sheath, contributing to underestimation in photographic measurements of arterial stumps. Moreover, visible venous spasm with caliber shrinking has been also noted at surgery by all surgeons, while this was not seen with arteries. Additionally, there may be a potential effect of nerve denudation of blood vessels during the D3 surgery and consequently a change in vascular tone. At the same time, the effect of cardiac cycles on arterial pulsatility, thus affecting arterial calibers, can also add variability to the data.

While virtual 3D-imaging, conveyed on a 2-dimensional screen, can provide detailed anatomical information, 3D printed models can become a superior complementary tool for better clinician–patient communication, diagnostics, treatment, especially for surgical planning and

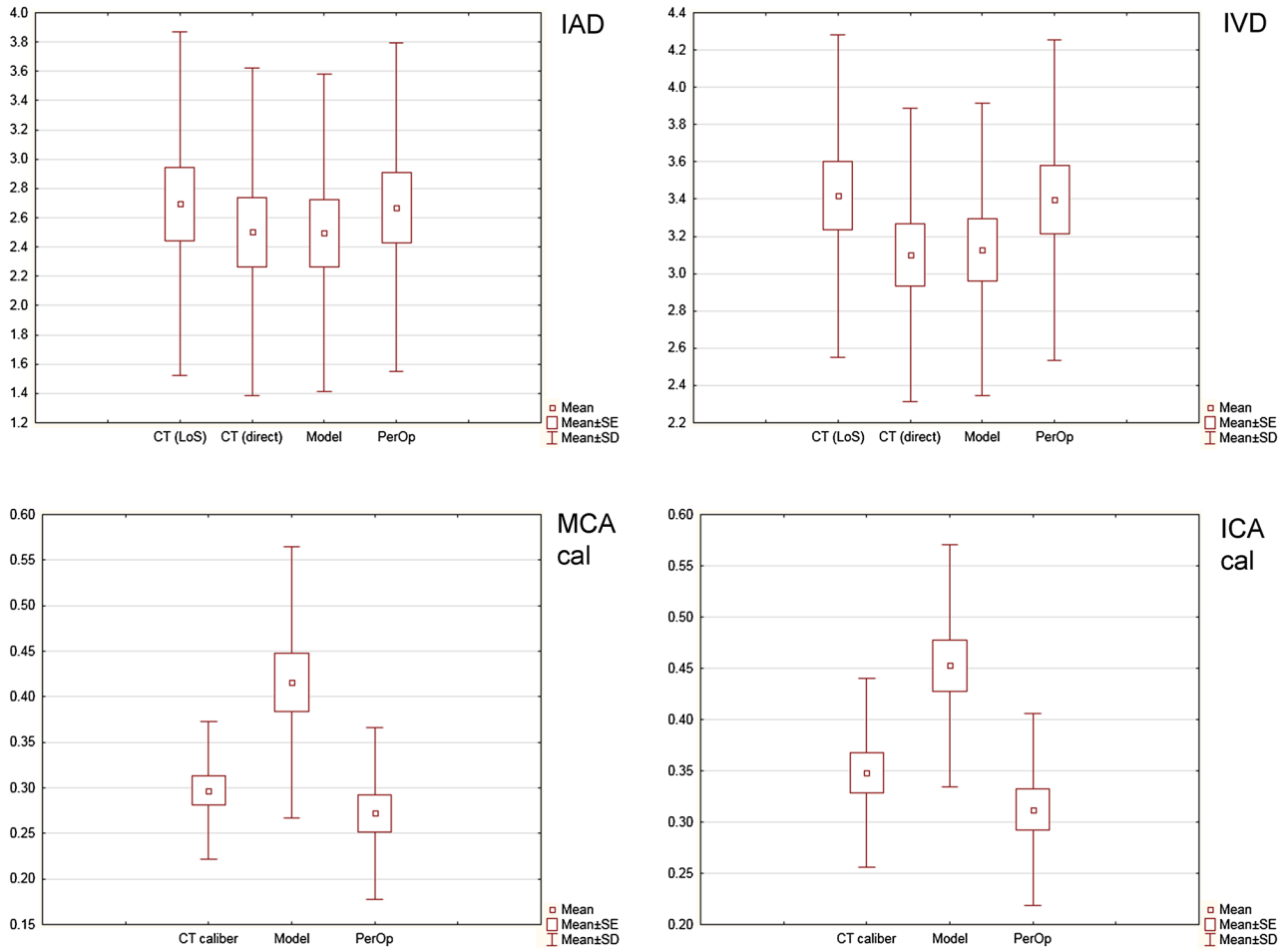

Fig. 4 Box & whisker plots of mean, standard error (SE) and standard deviation (SD) for variables IAD (inter-arterial distance), intervenous distance (IVD), middle colic artery caliber (MCAcal), and ileocolic artery caliber (ICAcal). Intervascular distances in centimeters and arterial calibers in millimeters

Table 1 Correlation matrix of linear parameters inter-arterial distances (IAD) and intervenous distance (IVD)

		IAD				IVD			
		CT (LoS)	CT (direct)	Model	PerOp	CT (LoS)	CT (direct)	Model	PerOp
	CT (LoS)								
r	CT (direct)	**0.968**				**0.973**			
	Model	**0.956**	**0.942**			**0.854**	**0.901**		
	PerOp	**0.779**	**0.720**	**0.840**		0.382	0.394	0.377	

"r"—Pearson's correlation coefficient

Bold—significant correlation

Table 2 Correlation matrix of middle colic artery (MCA) and ICA (Ileocolic) calibers

		MCAcal			ICAcal		
		CT	Model	PerOp	CT	Model	PerOp
r	CT						
	Model	**0.459**			**0.578**		
	PerOp	0.042	0.144		0.228	0.013	

"r"—Pearson's correlation coefficient

Bold—significant correlation

Table 3 Summary of material cost

Material	Cost ranges
Resin	13–21 USD
Isopropanol	1–5 USD
Building platform	6 USD
Resin tank	3–5 USD
Total cost per model	21–34 USD

Summary of material cost. Prices were converted from Norwegian crowns (NOK) to American dollars (USD) according to the recent currency exchange rate

navigational performance, as well as simulations and training [19]. Compared to the radiologist, the surgeon prefers to have a three-dimensional orientation when accessing the anatomy concerned, regardless of mode of access (open, laparoscopic, or robotic). In order to improve the quality of care, standardization of surgical procedures was proposed. The current standard for colonic cancer surgery is complete mesocolic excision (CME) with central vascular ligation (CVL) [20]. While the concept of standardization is encouraging, the results on the level of the CVL (which actually represents a surrogate endpoint for the extent of mesenterectomy/lymphadenectomy) in patients operated with CME, do not reflect the expected outcome. Subsequent studies published in respectable surgical journals have shown a consistency in incomplete surgical resection during CME with unexpectedly long post-resection arterial stumps, hence incomplete lymph node harvesting [21–23]. Possibly, this is one of the reasons that more radical surgery has the difficulty of proving better survival rates [24]. Equally important, the anatomical variability of the central mesenteric vasculature naturally discourages surgeons to operate in the area. Consequently, promotion of a standardized but personalized surgical approach that fits patients' individual vascular anatomy seems to be natural. It is, therefore, essential to investigate if these 3D printed models can accurately mirror individual patient vasculature and serve this purpose. Our results imply that this is the case and that they can become a visual tool to help the surgeon perform a correct central vascular ligation and surgical resection in oncologic cases.

Based on our results, the main limitation of this technology was the time and workload that are required to calibrate and maintain the 3D printer used, in order to obtain defect-free models in a continuous and efficient matter. Still, while the development of 3D printing technology, its availability and economic efficacy are, as of now, so variable, there is a positive movement towards faster, more inexpensive, and more efficient 3D printers [25].

Another constraint was the methodology used while measuring at surgery. While it can be expected to obtain adequate measurements during open surgery, one has to consider that it can be difficult to manually isolate and demonstrate the regions of interest even during laparotomy. Blood, multiple operative hands, and overstretching of vessels after they have been skeletonized can affect the measuring process with the naked eye. Moreover, the crude scale of the bendable paper ruler used to perform the measurements significantly hindered the precision of measurements. This is why photographing of the open abdomen and digital measuring was integrated in the methods. It is fair to add that maintaining camera positioning (directly above the patient) perpendicular to the operative table, during photographing, can also represent a challenge. While one can also argue that the number of cases used in this study is small, comparable studies on the role of 3D printing in abdominal surgery frameworks are based either on single case studies [26], or on a limited number of cases [27].

Another limitation of this 3D printing technology was the requirement for quality control and recognition of eventual malformed vascular shapes during the production of the 3D physical model. There is an ongoing debate on turning 3D printing into a multidisciplinary medical practice where radiologists, anatomists, and the referring physician/surgeon will have to take part in the manufacturing process to ensure anatomical accuracy [28]. In our case, while an anatomist was in charge of creating the 3D virtual models, the surgeon, who controlled the quality of the 3D physical models was the same one who obtained the peroperative intervascular measurements. In order to avoid any methodological bias, we applied the same morphometric approach to the virtual and physical models. The reference points on the arterial origins and venous terminations were identified on the 3D virtual models and closely followed on the corresponding 3D printouts. Moreover, these measuring methods have been standardized in previous studies measuring distances of corrosion cast derived from human cadavers [2, 4], which are comparable to CT-derived 3D printed models. Other authors [29] have also used a caliper for measuring distances between landmarks, but have additionally advocated the use of high-resolution imaging modality on 3D printed models. This could be a significant adjunct to model validation, but, in our view, it is questionable in the limited timeframe of clinical setting.

Integrating and using 3D printed models in the operative field require sterility. Previous studies have discussed various methods such as steam, low temperature, and chemical sterilization, and even the intrinsic sterilization properties of some 3D printers [30, 31]. According to the printer's own technical support team, the resin 3D models can be sterilized in an autoclave at 135 °C for 2 h without significant degradation, and this should be sufficient to ensure microbiocidal activity according to guidelines from the Centers of Disease Control and Prevention in USA (CDC) [25]. On the other

hand, using a sterile, transparent plastic bag containing the physical model can also be sufficient. This bag can also serve as a "collector" if fragile and minute pieces of the printout break and fall during intraoperative use.

Surgery of the future will likely include navigation systems to guide surgery based on individual patient anatomy. The 3D physical models presented in this article fulfill the requirements needed to be the basis for preoperative planning and surgical navigation. Incorporating this technology for further research can probably improve short and long-term outcomes (operative time, blood loss, complication rates, and costs) and have an effect on survival rates in this patient group. Feedback from colorectal surgeons was positive, based on the tactile and visual properties of the model. Cognitive and technical benefits at surgery using this technology will be addressed in future articles. Lastly, 3D anatomical printouts should already be incorporated in medical education and surgical training, as a bridge to bring anatomical variability from clinics into classrooms in order to improve anatomical knowledge and increase awareness in personalized surgery [32].

Conclusion

This study shows acceptable dimensional correlations between 3D printed models, 3D virtual STL models, and authentic soft tissue anatomy of the central mesenteric vessels. These results can serve as an endorsement for the medical practitioner that 3D printed on-site models could become a routine visual aid before and during surgery.

Acknowledgements We thank Dr. Yngve Thorsen for his valuable support, as a member of our research team.

Compliance with ethical standards

Disclosures Drs. Javier A. Luzon, Bjarte T. Andersen, Bojan V. Stimec, Jean H. D. Fasel, Arne O. Bakka, Airazat M. Kazaryan, Dejan Ignjatovic have no conflicts of interest or financial ties to disclose.

References

1. Hurst EJ (2016) 3D printing in healthcare: emerging applications. J Hosp Librariansh 16(3):255–267. https://doi.org/10.1080/15323269.2016.1188042
2. Bergamaschi R, Ignjatovic D (2000) More than two structures in Calot's triangle: a postmortem study. Surg Endosc 14(4):354–357
3. Ignjatovic D, Bergamaschi R (2002) Anatomical rationale for spleen salvage by lobe/segment dearterialization in inferior pole spleen injury during left hemicolectomy: a post-mortem study. Tech Coloproctol 6(2):93–95. https://doi.org/10.1007/s10151020020
4. Ignjatovic D, Stimec B, Finjord T, Bergamaschi R (2004) Venous anatomy of the right colon: three-dimensional topographic mapping of the gastrocolic trunk of Henle. Tech Coloproctol 8(1):19–21. https://doi.org/10.1007/s10151-004-0045-9
5. Sakata S, Watson MO, Grove PM, Stevenson AR (2016) The conflicting evidence of three-dimensional displays in laparoscopy: a review of systems old and new. Ann Surg 263(2):234–239. https://doi.org/10.1097/sla.0000000000001504
6. Malik HH, Darwood ARJ, Shaunak S, Kulatilake P, El-Hilly AA, Mulki O, Baskaradas A (2015) Three-dimensional printing in surgery: a review of current surgical applications. J Surg Res 199(2):512–522. https://doi.org/10.1016/j.jss.2015.06.051
7. Micallef J, SpringerLink (2015) Beginning design for 3D printing. Technology in action. Imprint, Apress
8. Ibrahim D, Broilo TL, Heitz C, de Oliveira MG, de Oliveira HW, Nobre SMW, Dos Santos Filho JHG, Silva DN (2009) Dimensional error of selective laser sintering, three-dimensional printing and PolyJet models in the reproduction of mandibular anatomy. J Cranio-Maxillo-Facial Surg 37(3):167. https://doi.org/10.1016/j.jcms.2008.10.008
9. George E, Liacouras P, Rybicki FJ, Mitsouras D (2017) Measuring and establishing the accuracy and reproducibility of 3D printed medical models. Radiographics 37(5):1424–1450. https://doi.org/10.1148/rg.2017160165
10. Martelli N, Serrano C, van Den Brink H, Pineau J, Prognon P, Borget I, El Batti S (2016) Advantages and disadvantages of 3-dimensional printing in surgery: a systematic review. Surgery 159(6):1485. https://doi.org/10.1016/j.surg.2015.12.017
11. Lee SD, Lim S-B (2009) D3 lymphadenectomy using a medial to lateral approach for curable right-sided colon cancer. Int J Colorectal Dis 24(3):295–300. https://doi.org/10.1007/s00384-008-0597-7
12. Nesgaard JM, Stimec BV, Bakka AO, Edwin B, Ignjatovic D (2015) Navigating the mesentery: a comparative pre- and peroperative visualization of the vascular anatomy. Colorectal Dis 17(9):810–818. https://doi.org/10.1111/codi.13003
13. George E, Barile M, Tang A, Wiesel O, Coppolino A, Giannopoulos A, Mentzer S, Jaklitsch M, Hunsaker A, Mitsouras D (2017) Utility and reproducibility of 3-dimensional printed models in pre-operative planning of complex thoracic tumors. J Surg Oncol 116(3):407–415. https://doi.org/10.1002/jso.24684
14. Torres IO, De Luccia N (2017) A simulator for training in endovascular aneurysm repair: the use of three dimensional printers. Eur J Vasc Endovasc Surg 54(2):247–253. https://doi.org/10.1016/j.ejvs.2017.05.011
15. Guyton AC, Hall JE (2011) Guyton & Hall physiology review, 2nd edn. edn. Elsevier Saunders, Philadelphia
16. Mescher A (2016) Junqueira's basic histology: text and atlas. Basic histology (review questions), 14th edn. McGraw-Hill Education LLC, New York
17. McGregor AD (1987) Prediction of internal arterial diameter from measurement of external diameter. Ann Plast Surg 19(3):217–218
18. Faury G, Maher GM, Li DY, Keating MT, Mecham RP, Boyle WA (1999) Relation between outer and luminal diameter in cannulated arteries. Am J Physiol 277(5 Pt 2):H1745–H1753
19. Fasel J, Aguiar D, Kiss-Bodolay D, Montet X, Kalangos A, Stimec B, Ratib O (2016) Adapting anatomy teaching to surgical trends: a combination of classical dissection, medical imaging, and 3D-printing technologies. Surg Radiol Anat 38(3):361–367. https://doi.org/10.1007/s00276-015-1588-3
20. Hohenberger W, Weber K, Matzel K, Papadopoulos T, Merkel S (2009) Standardized surgery for colonic cancer: complete mesocolic excision and central ligation–technical notes and outcome. Colorectal Dis 11(4):354–364. https://doi.org/10.1111/j.1463-1318.2008.01735.x
21. Spasojevic M, Stimec BV, Gronvold LB, Nesgaard JM, Edwin B, Ignjatovic D (2011) The anatomical and surgical consequences of

right colectomy for cancer. Dis Colon Rectum 54(12):1503–1509. https://doi.org/10.1097/DCR.0b013e318232116b
22. Kaye TL, West NP, Jayne DG, Tolan DJ (2016) CT assessment of right colonic arterial anatomy pre and post cancer resection—a potential marker for quality and extent of surgery? Acta Radiol (Stockholm, Sweden: 1987) 57(4):394–400. https://doi.org/10.1177/0284185115583033
23. Munkedal DLE, Rosenkilde M, Nielsen DT, Sommer T, West NP, Laurberg S (2017) Radiological and pathological evaluation of the level of arterial division after colon cancer surgery. Colorectal Dis 19(7):O238–O245. https://doi.org/10.1111/codi.13756
24. Willaert W, Ceelen W (2015) Extent of surgery in cancer of the colon: is more better? World J Gastroenterol 21(1):132–138. https://doi.org/10.3748/wjg.v21.i1.132
25. Hoang D, Perrault D, Stevanovic M, Ghiassi A (2016) Surgical applications of three-dimensional printing: a review of the current literature & how to get started. Ann Transl Med 4(23):456. https://doi.org/10.21037/atm.2016.12.18
26. Garcia-Granero A, Sanchez-Guillen L, Fletcher-Sanfeliu D, Flor-Lorente B, Frasson M, Sancho Muriel J, Alvarez Serrado E, Pellino G, Grifo Albalat I, Giner F, Roca Estelles MJ, Esclapez Valero P, Garcia-Granero E (2018) Application of three-dimensional printing in laparoscopic dissection to facilitate D3-lymphadenectomy for right colon cancer. Tech Coloproctol 22(2):129–133. https://doi.org/10.1007/s10151-018-1746-9
27. Chen Y, Li H, Wu D, Bi K, Liu C (2014) Surgical planning and manual image fusion based on 3D model facilitate laparoscopic partial nephrectomy for intrarenal tumors. World J Urol 32(6):1493–1499. https://doi.org/10.1007/s00345-013-1222-0
28. Mitsouras D, Liacouras P, Imanzadeh A, Giannopoulos AA, Cai T, Kumamaru KK, George E, Wake N, Caterson EJ, Pomahac B, Ho VB, Grant GT, Rybicki FJ (2015) Medical 3D printing for the radiologist. Radiographics 35(7):1965–1988. https://doi.org/10.1148/rg.2015140320
29. Leng S, McGee K, Morris J, Alexander A, Kuhlmann J, Vrieze T, McCollough C, Matsumoto J (2017) Anatomic modeling using 3D printing: quality assurance and optimization. 3D Print Med 3 (1):1–14. https://doi.org/10.1186/s41205-017-0014-3
30. Rankin TM, Giovinco NA, Cucher DJ, Watts G, Hurwitz B, Armstrong DG (2014) Three-dimensional printing surgical instruments: are we there yet? J Surg Res. https://doi.org/10.1016/j.jss.2014.02.020
31. Neches RY, Flynn KJ, Zaman L, Tung E, Pudlo N, Ahluwalia A (2016) On the intrinsic sterility of 3D printing. Peer J. https://doi.org/10.7717/peerj.2661
32. Li C, Kui C, Lee E, Sang Ho C, Hei Sunny Hei S, Wu W, Wong WT, Voll J, Li G, Liu T, Yan B, Chan J, Tse G, Keenan I (2017) The role of 3D printing in anatomy education and surgical training: a narrative review. MedEdPublish 6(2):31. https://doi.org/10.15694/mep.2017.000092

Affiliations

Javier A. Luzon[1,2] · Bjarte T. Andersen[3] · Bojan V. Stimec[4] · Jean H. D. Fasel[4] · Arne O. Bakka[1,2] · Airazat M. Kazaryan[2,5] · Dejan Ignjatovic[1,2]

1 Faculty of Medicine, Institute of Clinical Medicine, University of Oslo, Oslo, Norway

2 Division of Surgery, Department of Digestive Surgery, Akershus University Hospital, Lørenskog, Norway

3 Department of Gastroenterological Surgery, Østfold Hospital Trust, Sarpsborg, Norway

4 Anatomy Sector, Department of Cell Physiology and Metabolism, Faculty of Medicine, University of Geneva, Geneva, Switzerland

5 Department of Surgery №1, Yerevan State Medical University After M. Heratsi, Yerevan, Armenia